Reinforcing epoxy nanocomposites with functionalized carbon nanotubes via biotin-streptavidin interactions

Rouhollah Dermanaki Farahani[a], Hamid Dalir[a], Vincent Le Borgne[b], Loick. A. Gautier[b], My Ali El Khakani[b], Martin Lévesque[a], and Daniel Therriault[a]*

[a]Laboratory of Multiscale Mechanics, Center for applied research on polymers (CREPEC), École Polytechnique de Montreal, C.P. 6079, succ. Centre-Ville, Montreal (QC), H3C 3A7 (Canada)

[b]Institut National de la Recherche Scientifique, INRS-Énergie, Matériaux et Télécommunications, 1650 Blvd. Lionel-Boulet, Varennes (QC), J3X 1S2 (Canada)

* Corresponding author:

Phone: 1-514-340-4711 x4419; Fax: 1-514-340-4176;

E-mail: daniel.therriault@polymtl.ca

Abstract

We report on the preparation of nanocomposites consisting of biofunctionalized single-walled carbon nanotubes (BF-SWCNTs) reinforcing an ultraviolet curable epoxy polymer by means of biotin-streptavidin interactions. The as-produced laser ablation SWCNTs are biofunctionalized via acid oxidization based purification process and non-covalent functionalization using surfactant, followed by grafting the resulting nanotubes with biomolecules. The biotin-grafted nanotubes are capable of interacting with epoxy groups in presence of streptavidin molecules by which chemical bridges between BF-SWCNTs and epoxy matrix are formed. The biomolecules grafted to the nanotubes surface not only facilitate the load transfer, but also improve the nanotube dispersion into the epoxy matrix, as observed by optical imaging and scanning electron microscopy. Mechanical characterization on the nanocomposite microfibers demonstrates considerable enhancement in both strength (by 76%) and modulus (by 93%) with the addition of only 1 wt.% of BF-SWCNTs. The electrical measurements reveal a clear change in electrical conductivity of nanocomposite microfibers reinforced with 1 wt.% of BF-SWCNTs in comparison to the microfibers containing solely purified carbon nanotubes. These multifunctional nanocomposite materials could be used to fabricate macro and microstructures

for a wide variety of applications such as high strength polymer nanocomposite and potential easily-manipulated biosensors.

Keywords: A. Carbon nanotube, surface modification, A. Nanocomposite, UV-assisted direct-write

1. Introduction

Nanomaterials, such as single-walled carbon nanotubes (SWCNTs), are increasingly used to achieve multifunctional capabilities where they serve as an effective structural reinforcement, as well as large-surface platform for sensing purposes [1,2]. Owing to their high mechanical[3] and electrical [4] properties, SWCNTs show a strong potential for reinforcing polymers for a wide variety of applications such as high-performance structural composites [5,6], electromechanical actuators and sensors[7], non-destructive life prediction technology and shape memory polymers [8]. When compared to other polymer nanocomposites, nanotube-reinforced epoxy systems could exhibit high strength and multifunctional features for aircrafts and electronic products [6,9]. However, several fundamental challenges still have to be addressed in order to take full advantage of the excellent properties of the nanotubes. In particular, the ability to manipulate these entangled structures with their structurally smooth surface is required for their effective use in the development of nanodevices based on an individual nanotube or bulk nanotubes [10,11], as well as nanotube-reinforced nanocomposites [12-16].

The chemical treatment of carbon nanotubes surface significantly extends their potential for various applications. The surface functionalization of carbon nanotubes not only leads to their debundling, but also enables the design of an efficient interface to bond them to other active groups, like epoxy groups in nanocomposite materials. In particular, the purification induced covalent grafting of carboxylic groups at the surface of the nanotubes[17] as well as their non-covalent functionalization using surfactants like porphyrins[18] can be used to improve the reinforcing effect when compared to as-produced nanotubes. However, nanotube reinforcement

is still far from achieving its theoretical potential and new advances are needed for an efficient load transfer.

Functionalized nanotubes have been used for the immobilization of various biomolecules for biosensor applications [10]. Biomolecules bonded to functionalized nanotubes through functional groups are capable of interacting with other active biomolecules via reversible chemical bonding. Among these biomolecules, biotin-streptavidin bonding is known as one of the strongest interactions in nature [19,20]. Therefore, biotin-functionalized nanotubes could be used as a support to immobilize streptavidin molecules in biosensor applications. However, until now, most of the researches undertaken on using nanotubes in microelectronics have been limited to the use of an individual nanotube or bulk nanotubes. Due to the size order of an individual nanotube or their bulk physical state (i.e., powder of entangled structures), manufacturing and manipulation of these materials is quite challenging [10,11]. To address these difficulties, nanotubes have been added to a solution or a polymer matrix, suitable for use in electrospinning [21] and direct-write techniques [22]. Since fibers fabricated by electrospining need additional patterning processes, the ultraviolet (UV)-assisted direct-write assembly [23] could be an alternative to manufacture complex microstructures with desired patterns when an UV-curable epoxy resin is used as a matrix.

Here, we report on the use of biotin-streptavidin interactions for further development of a multifunctional nanotube/epoxy composite system. This nanocomposite material was used for the fabrication of nanocomposite microfibers as an example of patterned microstructures for potential micro electromechanical systems (MEMS). Figure 1 shows the schematic of the fabrication process of nanocomposite microfibers suspended between two rectangular pads of nanocomposite by means of UV-assisted direct-write technique. To fabricate the nanocomposites, the SWCNTs were biofunctionalized via acidic treatment and non-covalent functionalization using surfactant, followed by grafting of biomolecules to chemically bridge

SWCNTs and epoxy matrix. The different steps of nanotubes functionalization were assessed using various structural characterization techniques. Finally, the effects of SWCNTs biofunctionalization and their dispersion on mechanical and electrical properties of the fabricated epoxy nanocomposite microfibers were studied to understand the nanocomposite structure-property relationship.

2. Experimental details

2.1. SWCNTs synthesis, purification and biofunctionalization

Single-walled carbon nanotubes were synthesized by using UV-laser ablation (248 nm, 20 ns, 400 mJ) of a Co/Ni-doped (1.2 at. %) graphite target pellet. The KrF-laser ablation was performed under a controlled argon atmosphere at a temperature of 1150°C through a 45° quartz window (more experimental details on the KrF-laser synthesis and effects of key growth parameters can be found elsewhere [24,25]). The as-produced SWCNTs condensed on a water-cooled collector, located outside of the hot zone of the furnace, onto which they formed a thick rubbery-like film. This SWCNTs mat was peeled off and subjected to subsequent chemical purification treatment. The chemical purification treatment consisted of three main successive steps, each of which is targeted a specific purification. First, the Soxhlet extraction in toluene (for 1h) was conducted on the as-produced SWCNTs to remove residual fullerenes and some disordered carbon nanostructures in the deposit. Second, the SWCNTs were treated by hydrogen peroxide (10%) at room temperature (for 24 h) in order to crack the graphitic shells surrounding the residual catalyst nanoparticles. Finally, HNO_3 (3M) oxidation was conducted to remove metal catalyst particles and covalently functionalize the SWCNTs by the attachment of carboxylic groups at their surface. These chemically P-SWCNTs were collected by vacuum filtration on alumina filters (pore size 20 nm) and after successive rinsing cycles.

The desired amounts of P-SWCNTs and 1,3-diaminopropane 99% (D23602, Sigma-Aldrich), with a proportion of 1g P-SWCNTs/5 mL 1,3-diaminopropane 99%, were added to a solution of 0.1 mM of zinc protoporphyrin IX (ZnPP, Sigma-Aldrich) in methanol. The suspension was sonicated in an ultrasonic bath (Ultrasonic cleaner 8891, Cole-Parmer) for 1 h. After ultrasonication, the mixture was shaken using a mixer/shaker (Spex CertiPrep 8000M Mixer/Mill) for 12 h at room temperature. The Soxhlet extraction for 2 h with methanol was performed on the aminated P-SWCNTs to remove any unreacted amine. The aminated P-SWCNTs were then added into a solution of 30 mL methanol containing desired amounts of biotin and N,N'-diisopropylcarbodiimide 99% (DIC, D125407, Sigma-Aldrich) with a proportion of 1g biotin/5 mL DIC. Biotinylation of the aminated P-SWCNTs were subsequently performed by shaking the resulting mixture using the mixer/shaker for 12 h at room temperature. Finally, these biotinylated nanotubes were washed with methanol twice, followed by rinsing with distilled water several times to remove any unreacted biotin.

2.2. SWCNTs characterization

The KrF-laser synthesized SWCNTs were systematically characterized by various techniques before and after their chemical purification and functionalization. Their Raman spectra were acquired at room temperature in the 100 - 2000 cm^{-1} spectral region under ambient conditions using a back-scattering geometry on a microRaman microscope (Renishaw Imaging Microscope Wire TM) with a 50× objective. A 514.5 nm (2.41 eV) line from an air cooled Ar+ laser was used for excitation radiation. The chemical bonding states of the SWCNTs (before and after chemical purification) were analyzed by means of X-ray photoelectron spectroscopy (XPS) using the Cu K_{α} monochromatic radiation (1486.6 eV) of an ESCALAB 200I-XL spectrophotometer. The purified, aminated and biotinylated SWCNTs were characterized by FT-IR (Digilab FTS7000) in order to characterize the chemical components attached to the

surface of the nanotubes and assess the biofunctionalization procedure. Finally, the nanostructural characteristics of as-produced, P-SWCNTs and BF-SWCNTs were directly examined by transmission electron microscopy (TEM) using a Jeol JEM-2100F (FEG-TEM, 200 kV) microscope.

2.3. Nanocomposite preparation

The nanocomposite materials were prepared by mixing an Ultraviolet curable epoxy (UV-epoxy, UVE, UV15DC80, Master Bond Inc.) and either P-SWCNTs or BF-SWCNTs (at two loads of 0.5 wt.% and 1 wt.%). The UV-epoxy used in this study was a special one-component dual cure (ultraviolet/heat curable) epoxy resin which contains a UV photo-initiator having a maximum absorption at 365 nm and a heat-initiator active in the 60 – 80°C range. Biotin and 1,3-diaminopropane 99% (1g biotin/5 mL 1,3-diaminopropane 99%) were stored in 30 mL acetone and ultrasonicated for 30 min. The desired amount of functionalized nanotubes was subsequently added to the solution. Then, the UV-epoxy was slowly mixed with the resulting solution over a magnetic stirring hot plate (Model SP131825, Barnstead international) at 50°C for 4 h. Finally, the streptavidin solution (1 mL 10 µg/mL, S4762, from streptomyces avidinii, Sigma-Aldrich) was slowly added to the nanocomposite mixture and stirred for 1 h. After stirring, the nanocomposite mixture was simultaneously sonicated and heated in the ultrasonication bath at 50°C for 2 h. The residual trace of solvent was evaporated by heating the nanocomposite mixture at 30°C for 12 h and at 50°C for 24 h in a vacuumed-oven (RK-52402, Cole Parmer). The biotin-streptavidin interaction is not affected by the temperature during the solvent evaporation process, since very specific and harsh conditions are required to break the strong biotin-streptavidin bond [19,20].

After evaporation of the solvent, the nanocomposites were passed through a very small gap in a three-roll mill mixer (Exakt 80E, Exakt Technologies) for final high shear mixing [26]. The

gaps between the rolls varied in three batch-wise progressing steps (10 passes each) with three different gaps at 25 µm, 10 µm and 5 µm, respectively. The speed of the apron roll was adjusted to 250 RPM. The final mixture was then degassed under vacuum for 12 h. For comparison purposes, the nanocomposites with P-SWCNTs were also prepared using the same mixing procedure.

2.4. Nanocomposite morphological characterization

For optical imaging purposes, ~20 µm-thick films of the nanocomposites were fabricated by direct deposition on a glass substrate by means of a computer-controlled robot (I & J2200-4, I & J Fisnar) that moves a dispensing apparatus (HP-7X, EFD) along the *x*, *y* and *z* axes [22,27]. The quality of the mixing was observed for the cured nanocomposite films using an optical microscope (BX-61, Olympus) and image analysis software (Image-Pro Plus V5, Media Cybernetics). Microtomed surface of the bulk nanocomposite samples were also observed using field emission scanning electron microscopy (FESEM JEOL, JSM-7600TFE) in order to observe the nanotube dispersion.

2.5. Nanocomposite electrical and mechanical characterizations

The ultraviolet-assisted direct-write technique [23] was used to fabricate nanocomposites microfibers in order to assess the reinforcing effects of P-SWCNTs and BF-SWCNTs in the epoxy matrix. Two parallel thick square pads of the nanocomposites with 6 mm gap were first fabricated by extruding the nanocomposites suspensions through a micro-nozzle (5127-0.25-B, Precision Stainless Steel Tips, EFD, internal diameter (*ID*) = 150 µm) over a glass substrate. Right after, the pads were in situ cured using the optical fibers collected the light from two high-intensity UV light-emitting diodes (LED, NCSU033A, Nichia). Three suspended microfibers were then fabricated between two pads made of the same material. The microfibers were cured using UV exposure while being extruded (Figure 1). The electrical properties of the

nanocomposite microfibers were characterized using a Keithley 4200 semiconductor parametric analyzer with silver electrodes sputtered on the pads. Mechanical properties (tensile modulus, strength and elongation at break) of the nanocomposites microfibers were measured in a dynamic mechanical analyzer (DMA, DMA2980, TA instruments) using a film tension clamp. The microfibers were tested with a constant loading rate adjusted to reach failure within 20 ± 3 s according to the ASTM D2256 standard. A minimum of five specimens from each nanocomposite sample were tested.

3. Results and Discussion

3.1. Nanotube structural characterization

Figure 2(a) shows typical Raman spectra of the KrF-laser synthesized SWCNTs before and after their chemical purification. The peaks located in the 100-300 cm^{-1} and the 1500-1600 cm^{-1} ranges are typical fingerprints of SWCNTs. The first peak is due to the radial breathing mode (RBM) of the SWCNTs while the second is associated with the tangential vibrations of the C atoms forming the nanotube surface (G band). The RBM peak centred around 182 cm^{-1} arises from SWCNTs with a diameter of 1.26 nm [28]. The D band (1340 cm^{-1}) is generally attributed to the presence of amorphous carbon (a-C) and/or disordered carbon (d-C). The G/D ratio is generally used to qualify the degree of purity of the nanotubes. Here, the G/D ratio is found to decrease for the purified SWCNTs (P-SWCNTs). This is in fact a consequence of the creation of defects on SWCNTs' surface by the nitric acid oxidation step in the purification process. This is further supported by XPS measurements shown in Figure 2(b). The main C 1s core level peak that arises from the C=C bonds is narrow in both samples at 284.5 keV. However, for P-SWCNTs, a shoulder appearing at 288 keV is also present in the spectrum. This component is attributed to the C-O-O carboxylic groups resulting from the covalent functionalization of the

nanotubes by the nitric acid treatment [29]. Based on the XPS results, it is fair to assume that the purification process led to carboxylic groups grafting onto the SWCNTs surfaces.

Figure 2(c) shows a typical TEM micrograph of the as-produced SWCNTs where the nanotubes are found to self assemble, most often into bundles with a diameter in the 5-20 nm range and lengths reaching up to few microns. Other structures, such as carbon-surrounded catalyst nanoparticles and/or graphitic nanostructures (i.e., dark spots in the micrograph) are also present. The various steps of purification are intended to remove residual metal catalyst nanoparticles and most of the undesired carbon forms (e.g., a-C, d-C, fullerenes). Figure 2(d) shows a typical TEM image of the P-SWCNTs. Nevertheless, one can still notice the presence of few dark spots that line the bundles. These are likely some residual catalyst nanoparticles, which were not entirely digested during the nitric acid oxidation treatment. Thermogravimetry analysis (TGA) measurements (not shown here) have demonstrated a substantial decrease (by more than 60%) in the concentration of residual catalyst in the P-SWCNTs samples, when compared to the as-produced SWCNTs.

FT-IR spectroscopy was also used to characterize the chemical components attached to the surface of SWCNTs. Figure 3(a) shows the FT-IR spectra of the functionalized SWCNTs at each step of the biofunctionalization process. The FT-IR spectrum of P-SWCNTs shows two specific bands at 1315 cm^{-1} and 1732 cm^{-1}, associated with carboxylic groups [30]. The aminated and biotinylated SWCNTs revealed an appearance of two new strong bands centered at 1450 cm^{-1} and 1479 cm^{-1}, confirming reactions between carboxylic and amino groups [31]. The FT-IR spectrum of biofunctionalized carbon nanotubes (i.e., biotinylated SWCNTs) shows appearance of two new broad peaks centered around at 1594 cm^{-1} and 1635 cm^{-1}, which are assigned to 2° amide I and amide II, respectively [31]. The original amide groups of biotin as well as the amide bonds formed between amino groups on the aminated SWCNTs and carboxylic groups on the biotin are believed to be responsible for the two new peaks. The

appearance of these peaks in the spectrum of biofunctionalized SWCNTs (BF-SWCNTs) proves the grafting of the active biotin groups on the nanotubes surfaces through covalent bonds [31]. A high resolution TEM image (Figure 3(b)) shows individual P-SWCNTs with a very clean surface. This figure permits the direct measurement of the nanotube diameters (1.1-1.3 nm). Finally, Figure 3(c) shows a high-resolution TEM image of a SWCNT covered with a rough-looking material, most likely biomolecules or a mixture of carbonaceous residue and biomolecules, suggesting the effective presence of the grafted biomolecules on the SWCNTs surface [13].

3.2. Morphology characterization

Figures 4(a) and 4(b) show optical micrographs of two representative nanocomposites films with 1 wt.% loading of P-SWCNTs and BF-SWCNTs, respectively. The observed dark spots are thought to be nanotubes aggregates or nanotubes entangled around other carbonaceous materials. For the P-SWCNTs (Figure 4(a)), the majority of the nanotube aggregates are in the sub-micron range but some micron-size aggregates with a diameter of up to ~1μm are also present. A drastic change of the size of the aggregates was observed for the nanocomposite film with the BF-SWCNTs (Figure 4(b)). The larger spots observed for the P-SWCNTs-reinforced nanocomposite film became smaller, to 0.7 μm diameter (in average) when the BF-SWCNTs were used. To further support the optical observations, the cross-section of the nanocomposites microfibers was also observed under scanning electron microscopy (SEM). Figures 4(c) and 4(d) show typical SEM images of the surface of nanocomposites with 1 wt.% loading of P-SWCNTs and BF-SWCNTs, respectively. In the purified SWCNT-reinforced nanocomposite, the nanotubes formed clusters and large aggregates (i.e., the bright spots). When the biofunctionalized SWCNTs were used, the large aggregates disappeared and it was difficult to spot clusters of SWCNTs. Based on all the above observations, the fairly uniform dispersion of

the nanotubes and their associated aggregates for both cases might be attributed to the effectiveness of the nanocomposite mixing procedure combining ultrasonication and three-roll mill mixing methods. Comparing the nanocomposites dispersion suggests that the presence of biomolecules at the nanotube-matrix interface prevented re-aggregation of nanotubes and improved the SWCNTs dispersion.

3.3. Mechanical properties

The effect of biofunctionalization of SWCNTs on the mechanical properties was assessed by tensile testing. Figure 5 shows the stress-strain curves along with their resulting histograms of the neat UV-curable epoxy (UV-epoxy) and its associated nanotube-reinforced nanocomposites, prepared either with the P-SWCNTs or BF-SWCNTs. Figure 5(a) shows an optical image of typical microfibers used in the tensile experiments and Figure 5(b) is a representative SEM image of a fiber cross-section after its fracture under tensile loading. The error bars on the histograms were calculated from the 95% confidence intervals on the mean value obtained from the measurements. When the BF-SWCNTs were added to the composite with 0.5 wt.% loading, the average modulus showed an increase of 59% compared to that of the neat resin and an increase of 19% when compared to that of the nanocomposite reinforced with the same nanotube loading of P-SWCNTs. The improvement of modulus for the composites with 1 wt.% BF-SWCNTs loading were found to be 93% and 16% when compared to those of the neat resin and the P-SWCNTs-reinforced composites, respectively. The increased stiffness, from the neat epoxy resin to the nanocomposites, might be attributed to the proper dispersion as well as beneficial orientation of the nanotubes that may occur during the extrusion of the nanocomposite through the micronozzle [32]. For both nanotube loadings, BF-SWCNTs led to nanocomposites ~20% stiffer than that obtained with P-SWCNTs. The contribution of possible orientation in this higher stiffness is unlikely, since all nanocomposite microfibers were

fabricated under the same extrusion conditions. Therefore, the further improvement of stiffness for the BF-SWCNT-based nanocomposites is most likely attributed to the increased effective aspect ratio of the BF-SWCNTs as a consequence of their better dispersion.

The average failure strength of the P-SWCNTs- and BF-SWCNTs-reinforced nanocomposite was also improved with the addition of nanotubes. The incorporation of 0.5 wt.% BF-SWCNTs to the epoxy matrix increased its strength by approximately 50%. The nanocomposite with 1 wt.% BF-SWCNTs showed further enhancement (by 75%). For both nanotube loadings, higher failure strength (up to 24%) was achieved for the composites reinforced with BF-SWCNTs when compared to the P-SWCNTs-reinforced composites. More interestingly, the strength of the nanocomposite microfibers containing 0.5 wt.% BF-SWCNTs was found to be very close to that of the 1 wt.% P-SWCNTs-reinforced nanocomposite microfibers. This relatively higher improvement could be attributed to a possible strong nanotube/matrix interfacial interaction and to a good dispersion of nanotubes with the presence of the biomolecules. Considering the quantity of the SWCNTs added, these improvements of both modulus and strength are among the highest improvements for epoxy composites reported so far, as compared in Table 1 [9,12,13].

3.4. Governing interaction mechanisms

The possible governing interaction mechanisms between nanotubes and epoxy matrix with the presence of biomolecules are schematized in Figure 6. The proposed mechanism can be interpreted in the light of the mechanisms proposed by Wang et al. [31] and Sun et al. [12]. The nanotube biofunctionalization begins with grafting (covalently and non-covalently) carboxylic and amine groups to the surface of SWCNTs (more details on the synthesis procedure are found in experimental section). Grafting biomolecules on the nanotubes surface relies on the carboxylic groups created during the nanotube purification and on the use of Zinc

protoporphyrin IX (ZnPP) molecules. ZnPP molecules can non-covalently interact with the nanotubes wall through π-π interactions [18,22]. It should be mentioned that the functionalization procedure used in this study is non-destructive to the sidewall by attaching functional groups to the nanotubes. Since the long acidic treatment can destroy the wall integrity and consequently affect the mechanical properties of the resulting nanocomposite, the duration of acidic treatment was effectively controlled in our purification process. The carboxylic groups are capable of interacting with the amine groups and could contribute to further grafting of biomolecules to the surface of nanotubes. Streptavidin molecules offer four active sites which are equally capable of binding with biotin. The streptavidin was added to the BF-SWCNTs mixture in the presence of epoxy resin in order to avoid possible consumption of their four active sites by BF-SWCNTs, since they should be still-active to bridge between BF-SWCNTs and epoxy matrix (Figure 6b). The proposed interaction mechanism between streptavidin, biotin and epoxy resin on the right side of Figure 6b (i.e., epoxy side) was inspired from the work done by Wang et al. [31]. Therefore, a very strong nanotube-epoxy cross-linked network could be obtained by the action of active streptavidin that binds to other biotin molecules, which are attached to either epoxy groups or BF-SWCNTs.

The formation of such chemical bonding is believed to be responsible for the reasonable increase of failure strength obtained for the BF-SWCNTs-reinforced nanocomposites. It is worth noting that the average failure strain of 1 wt.% BF-SWCNTs-reinforced nanocomposite microfibers showed a slight increase (by 19%) in comparison to that of neat epoxy microfibers. Considering the flexibility of SWCNTs and their highly elastic behavior, the improvement of failure strain might be another proof of strong interfacial interaction [9]. Another contribution might come from stretching the curved and entangled nanotubes during the mechanical solicitation [9]. These factors could contribute to the increased failure elongation only when the nanotubes are well-bonded to the matrix through strong interfacial interactions. Therefore, the

BF-SWCNTs could be used not only as a strong reinforcement but also to slightly improve failure strain and thus to increase toughening properties and impact resistance of intrinsically brittle epoxies as reported in the literature [9,12]. The toughening effect of the nanotubes might be further evolved from the non-linear response of the nanocomposites under strain [32], since the response of the neat epoxy resin is linearly elastic (Figure 5c). It has been reported that carbon nanotubes could promote effective toughening mechanisms such as crack bridging and shear banding, although these reasons were not experimentally verified here. When compared to current toughening methods such as rubber modification of epoxy resins which may decrease their other mechanical properties, well-bonded carbon nanotubes confer an extra benefit without sacrificing other properties. This benefit can be translated to epoxy-based traditional structural composites in order to improve the epoxy matrix toughness of composite laminates in which nanotubes are added to the epoxy matrix. Thus, the toughening affect might be the most important advantage of nanomodification in this new class of composites which are known as multiscale composites.

3.5. Electrical conductivity

The effect of biofunctionalization of the nanotubes on electrical conductivity was studied. The electrical conductivity of the P-SWCNTs and BF-SWCNTs-reinforced composite microfibers was characterized upon voltage application between two silver-coated pads. Figure 7 shows the measured current with respect to applied voltage (I-V) curve of the nanocomposite microfibers for two different nanotubes loadings. Linear responses, with different slopes (R), of the currents versus the applied voltage were observed for all nanocomposite microfibers. For the microfibers with nanotube loading of 0.5 wt.%, the BF-SWCNTs were found to lead to slightly lower conductivities (by 19%), but this remains within the uncertainty of the measurements. At nanotube loading of 1 wt.%, the nanocomposite microfibers with BF-SWCNTs showed a

decrease of 129% in electrical conductance (i.e., *1/R*) when compared to that of P-SWCNTs-reinforced nanocomposite. The decrease of electrical conductivity might be attributed to the presence of streptavidin molecules that possibly act as a less-conductive layer surrounding the SWCNTs. The measured resistivity was decreased with the addition of more nanotubes (1 wt.%) through which more electrical percolation pathways should be formed. This could be described by the electrical conductivity mechanisms for the nanocomposites which are direct contact of nanotubes in their percolation pathways and/or electron tunneling between neighboring nanotubes at sufficiently close proximity [33]. Depending on nanotube loading, the contribution of these two mechanisms in the measured electrical conductivity varies. At the nanotube loading of 0.5 wt.%, electrons must travel through larger amounts of insulating epoxy matrix between the conductive nanotubes and the contribution of electron tunneling in the electrical conductivity is likely larger when compared to that of nanocomposites with 1 wt.% nanotubes. When more percolation conducting pathways are formed (at higher nanotube loadings), electrons conduct predominantly along the conductive nanotube pathways and thus, the effect of electron tunneling decreases [33]. For bio-functionalized nanotubes, the biomolecules might be placed between conductive nanotubes in their percolation pathways and affect the nanocomposite conductivity. Therefore, it is thought that the presence of biomolecules is more significant at higher nanotube concentrations and responsible for a clear change in the electrical conductivity of the nanocomposite microfibers containing 1 wt.% of SWCNTs. This phenomenon has been used for potential biosensor applications where streptavidin molecules are detected by their attachment to the surface of biotin-functionalized nanotubes [31,34].

4. Conclusions

The surface biofunctionalization of SWCNTs and the utilization of an efficient mixing procedure enabled the full integration of nanotubes within an epoxy matrix. Although the

nanotube dispersion and mechanical properties of the nanocomposite reinforced with P-SWCNTs were reasonably improved in comparison to the neat epoxy, subsequent grafting of biotin molecules to the P-SWCNTs led to a fairly good dispersion and further enhancement in their reinforcing effect. The failure strength of nanocomposite microfibers reinforced with 1 wt.% of BF-SWCNTs showed an increase of 76% when compared to that of pure resin and an increase of 25% when compared to that of the nanocomposite reinforced with P-SWCNTs, indicating the effectiveness of biofunctionalization to facilitate load transfer. The nanocomposite high strength provided by the biomolecules interactions make these multifunctional nanocomposites a good choice for the fabrication of high-performance nanocomposite-based devices in micro electromechanical systems and microelectronics. Considering the ability to change the electrical conductivity of the microfibers under mechanical disturbances and also by capturing biomolecules, the utilization of these multifunctional nanocomposite materials enables the fabrication of easily-manipulated strain sensors and porous microfibers or 3D complex patterns as solid support materials for potential biosensor applications.

Acknowledgements

The authors acknowledge the financial support from FQRNT (Le Fonds Québécois de la Recherche sur la Nature et les Technologies). Prof. El Khakani acknowledges also the financial support from NSERC (National Science Engineering Research Council of Canada) and Plasma-Québec (le Réseau Stratégique du FQRNT sur la Science et Technologies des Plasmas). The authors would like to thank the technical support of Dr. K. Laaziri from Laboratoire de recherche sur les nanostructures et interfaces conductrices for the electrical measurements.

References

[1] Dharap P, Li ZL, Nagarajaiah S, Barrera EV. Nanotube film based on single-wall carbon nanotubes for strain sensing. Nanotechnology. 2004;15(3):379-382.
[2] Su PG, Huang SC. Electrical and humidity sensing properties of carbon nanotubes-SiO2-poly (2-acrylamido-2-methylpropane sulfonate) composite material. Sensors and Actuators B-Chemical. 2006;113(1):142-149.
[3] Qian D, Wagner GJ, Liu WK, Yu M-F, Ruoff RS. Applied Mechanical Review. 2002;55(6):495-532.
[4] Tans SJ, Devoret MH, Dai HJ, Thess A, Smalley RE, Geerligs LJ, et al. Individual single-wall carbon nanotubes as quantum wires. Nature. 1997;386(6624):474-477.
[5] Coleman JN, Khan U, Gun'ko YK. Mechanical reinforcement of polymers using carbon nanotubes. Advanced Materials. 2006;18(6):689-706.
[6] Ear Y, Silverman E. Challenges and opportunities in multifunctional nanocomposite structures for aerospace applications. MRS Bulletin. 2007;32(4):328-334.
[7] Mirfakhrai T, Krishna-Prasad R, Nojeh A, Madden JDW. Electromechanical actuation of single-walled carbon nanotubes: an ab initio study. Nanotechnology. 2008;19(31):1-8.
[8] Sahoo NG, Jung YC, Yoo HJ, Cho JW. Influence of carbon nanotubes and polypyrrole on the thermal, mechanical and electroactive shape-memory properties of polyurethane nanocomposites. Composites Science and Technology. 2007;67(9):1920-1929.
[9] Zhu J, Peng HQ, Rodriguez-Macias F, Margrave JL, Khabashesku VN, Imam AM, et al. Reinforcing epoxy polymer composites through covalent integration of functionalized nanotubes. Advanced Functional Materials. 2004;14(7):643-648.
[10] Atashbar MZ, Bejcek B, Singamaneni S, Santucci S. Carbon nanotube based biosensors. Proceedings of the IEEE Sensors 2004, 1-3:1048-1051.
[11] Kong J, Franklin NR, Zhou CW, Chapline MG, Peng S, Cho KJ, et al. Nanotube molecular wires as chemical sensors. Science. 2000;287(5453):622-625.
[12] Sun L, Warren GL, O'Reilly JY, Everett WN, Lee SM, Davis D, et al. Mechanical properties of surface-functionalized SWCNT/epoxy composites. Carbon. 2008;46(2):320-328.
[13] Wang S, Liang R, Wang B, Zhang C. Reinforcing polymer composites with epoxide-grafted carbon nanotubes. Nanotechnology. 2008;19(8):1-7.
[14] Wang SR, Liang ZY, Liu T, Wang B, Zhang C. Effective amino-functionalization of carbon nanotubes for reinforcing epoxy polymer composites. Nanotechnology. 2006;17(6):1551-1557.
[15] Zhao JX, Ding YH. Functionalization of single-walled carbon nanotubes with metalloporphyrin complexes: A theoretical study. Journal of Physical Chemistry C. 2008;112(30):11130-11134.
[16] Zhu J, Kim JD, Peng HQ, Margrave JL, Khabashesku VN, Barrera EV. Improving the dispersion and integration of single-walled carbon nanotubes in epoxy composites through functionalization. Nano Letters. 2003;3(8):1107-1113.
[17] Chen J, Hamon MA, Hu H, Chen YS, Rao AM, Eklund PC, et al. Solution properties of single-walled carbon nanotubes. Science. 1998;282(5386):95-98.
[18] Nakashima N, Fujigaya T. Fundamentals and applications of soluble carbon nanotubes. Chemistry Letters. 2007;36(6):692-697.
[19] Holmberg A, Blomstergren A, Nord O, Lukacs M, Lundeberg J, Uhlen M. The biotin-streptavidin interaction can be reversibly broken using water at elevated temperatures. Electrophoresis. 2005;26(3):501-510.
[20] Laitinen OH, Hytonen VP, Nordlund HR, Kulomaa MS. Genetically engineered avidins and streptavidins. Cellular and Molecular Life Sciences. 2006;63(24):2992-3017.
[21] Patel AC, Li SX, Yuan JM, Wei Y. In situ encapsulation of horseradish peroxidase in electrospun porous silica fibers for potential biosensor applications. Nano Letters. 2006;6(5):1042-1046.

[22] Lebel LL, Aissa B, El Khakani MA, Therriault D. Preparation and mechanical characterization of laser ablated single-walled carbon-nanotubes/polyurethane nanocomposite microbeams. Composites Science and Technology. 2010;70(3):518-524.
[23] Lebel LL, Aissa B, El Khakani MA, Therriault D. Ultraviolet-Assisted Direct-Write Fabrication of Carbon Nanotube/Polymer Nanocomposite Microcoils. Advanced Materials. 2010;22(5):592-596.
[24] Braidy N, El Khakani MA, Botton GA. Effect of laser intensity on yield and physical characteristics of single wall carbon nanotubes produced by the Nd : YAG laser vaporization method. Carbon. 2002;40(15):2835-2842.
[25] Le Borgne V, Aissa B, Mohamedi M, Kim YA, Endo M, El Khakani MA. Pulsed KrF-laser synthesis of single-wall-carbon-nanotubes: effects of catalyst content and furnace temperature on their nanostructure and photoluminescence properties, 2011;13 (11):5759-5768.
[26] Thostenson ET, Chou TW. Processing-structure-multi-functional property relationship in carbon nanotube/epoxy composites. Carbon. 2006;44(14):3022-3029.
[27] Therriault D, Shepherd RF, White SR, Lewis JA. Fugitive inks for direct-write assembly of three-dimensional microvascular networks. Advanced Materials. 2005;17(4):395-399.
[28] Bachilo SM, Strano MS, Kittrell C, Hauge RH, Smalley RE, Weisman RB. Structure-assigned optical spectra of single-walled carbon nanotubes. Science. 2002;298(5602):2361-2366.
[29] Okpalugo TIT, Papakonstantinou P, Murphy H, McLaughlin J, Brown NMD. High resolution XPS characterization of chemical functionalised MWCNTs and SWCNTs. Carbon. 2005;43(1):153-161.
[30] Bruneaux J, Therriault D, Heuzey MC. Micro-extrusion of organic inks for direct-write assembly. Journal of Micromechanics and Microengineering. 2008;18(11):1-8
[31] Wang D, Sun G, Xiang B, Chiou BS. Controllable biotinylated polyethylene-co-glycidyl methacrylate) (PE-co-GMA) nanofibers to bind streptavidin-horseradish peroxidase (HRP) for potential biosensor applications. European Polymer Journal. 2008;44(7):2032-2039.
[32] Moussaddy H, Farahani RD, El Khakani MA, Lévesque M, Therriault D. Mechanical properties of chemically-treated carbon nanotube nanocomposite microfibers: experimental and modeling studies. The second joint US-Canada conference on composites, 2011.
[33] Winey KI, Kashiwagi T, Mu MF. Improving electrical conductivity and thermal properties of polymers by the addition of carbon nanotubes as fillers. Mrs Bulletin. 2007;32(4):348-353.
[34] Sotiropoulou S, Chaniotakis NA. Carbon nanotube array-based biosensor. Analytical and Bioanalytical Chemistry. 2003;375(1):103-105.

Figures and Tables captions

Figure 1. Schematic representation of the UV-assisted direct-writing of nanocomposite microfibers: (a) nanocomposite extrusion through a capillary micronozzle by an applied pressure; fibers are partially cured shortly after extrusion under UV illumination, (b) close-up view of the microfibers, and (c) interfacial bonding between SWCNTs and epoxy matrix through biotin-streptavidin interactions.

Figure 2. (a) Raman spectra, (b) X-ray photoelectron spectra of as-produced (bottom) and purified (top) SWCNTs, (c) typical TEM image of as-produced SWCNTs, and (d) TEM image of P-SWCNTs.

Figure 3. (a) FT-IR spectra of (i) P-SWCNTs (bottom), (ii) aminated SWCNTs (middle), and (iii) biotinylated SWCNTs (BF-SWCNTs) (top), (b) high-resolution TEM image of a P-SWCNTs, and (c) high-resolution TEM image of a BF-SWCNTs.

Figure 4. Optical microscope images of a 20-μm thick film of the nanocomposite containing (a) 1 wt% P-SWCNTs and (b) 1 wt% BF-SWCNTs, (c) and (d) typical SEM images of the cross-section surface of the bulk nanocomposites containing 1 wt% P-SWCNTs and 1 wt% BF-SWCNTs, respectively.

Figure 5. Mechanical characterization of the nanocomposite materials: (a) optical image of a typical fabricated specimen consisting of three suspended fibers between two rectangular pads, (b) SEM image of fracture surface of a nanocomposite fiber, (c) typical stress–strain curves and (d) histograms of modulus, strength and failure strain of the pure UV-epoxy and its associated nanocomposites.

Figure 6. Schematics of (a) synthesis procedure of the BF-SWCNTs and (b) proposed interaction mechanisms governing the interaction of the BF-SWCNTs and the epoxy matrix by bridge formation through biotin-streptavidin interactions.

Figure 7. Measured current upon voltage application for the nanocomposite microfibers.

Table 1. Comparison of the mechanical properties improvements in our work with those reported in literature.

Table 1

SWCNTs type	SWCNTs wt.%	Processing method	Modulus (% increase)	Strength (% increase)	Ref.
NH_2-modified	1.0	Solution mixing	31	25	[9]
Amine-modified	1.0	Simple mixing	26	16	[12]
Epoxide-modified	1.0	Solution mixing	60	40	[13]
Carboxyl-modified	1.0	Shear mixing	24	-	[?]
NH_2-modified	0.1	Simple mixing	56	12	[?]
Fluorinated	1.0	Solution mixing	30	18	[?]
Purified	5.0	Solution mixing	0	7	[?]
Bio-functionalized	1.0	Solution & shear mixing	93	75	Present work

Figure 1

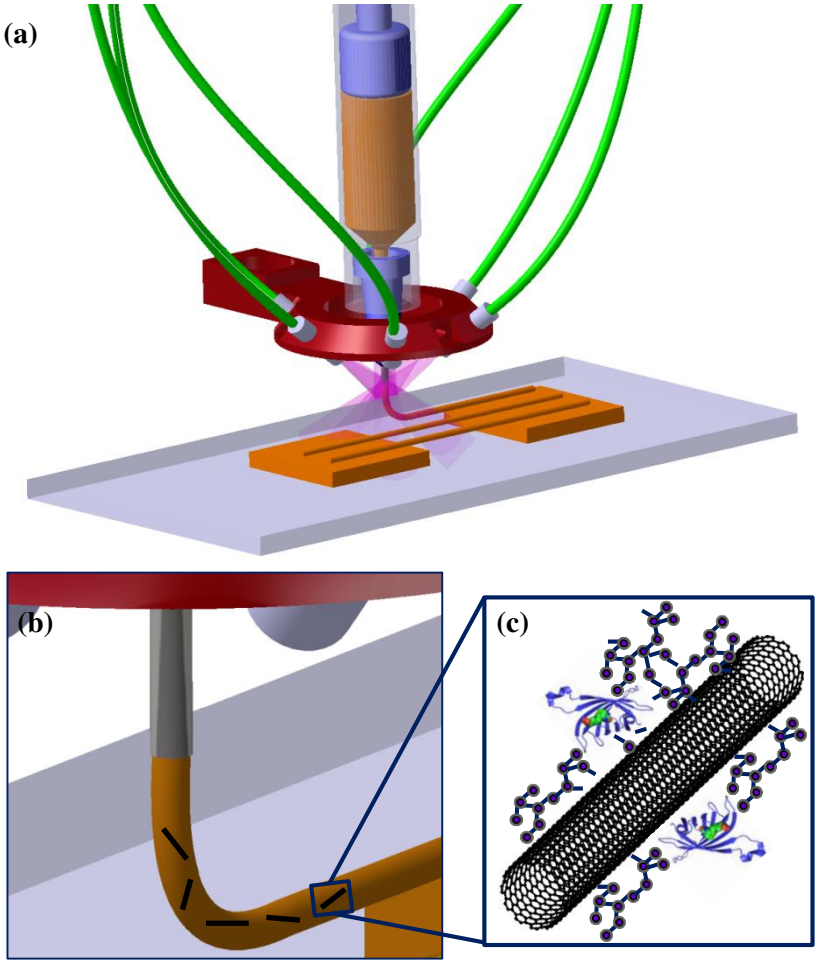

Figure 2

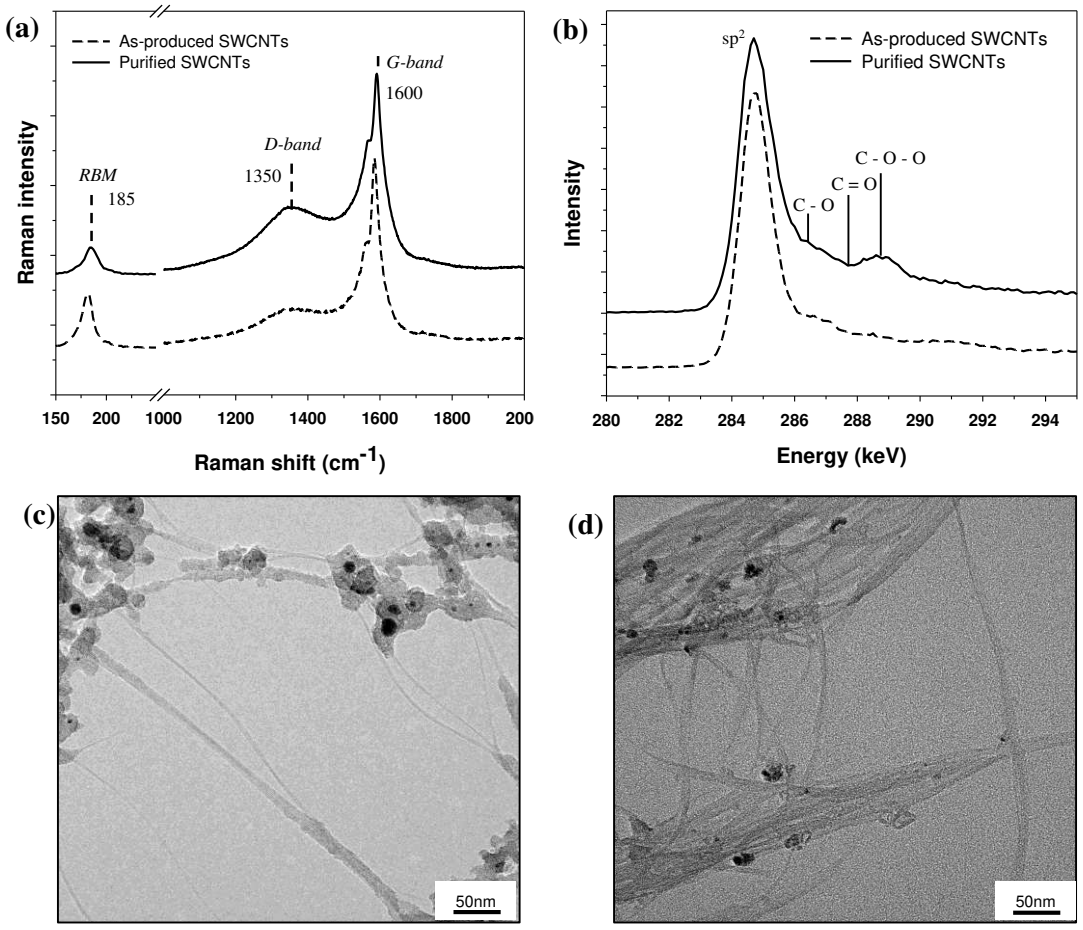

Figure 3

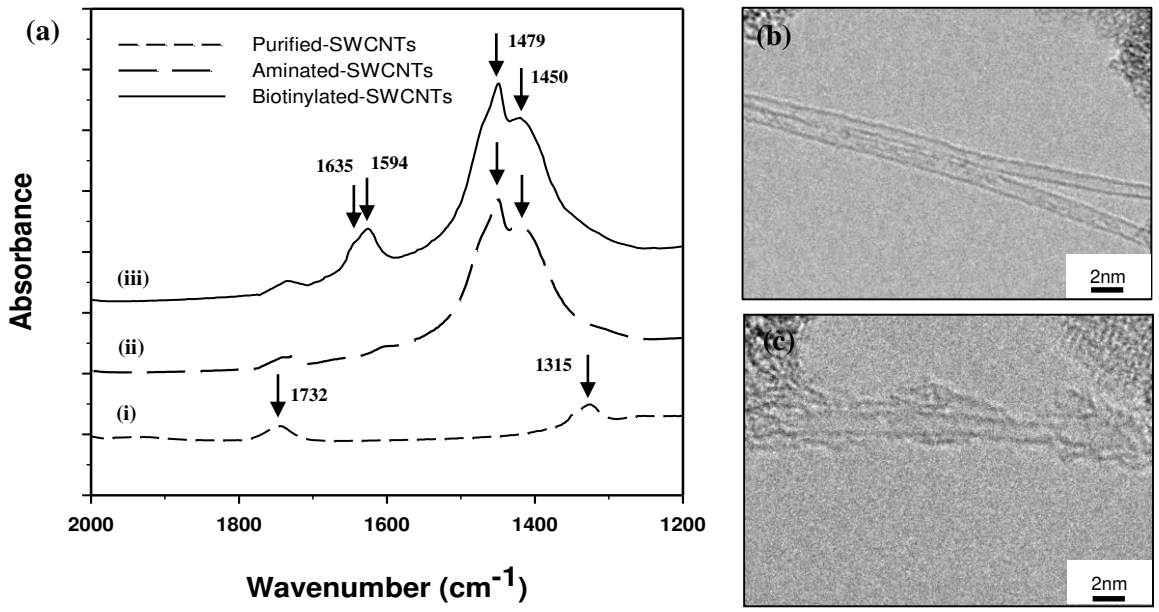

Figure 4

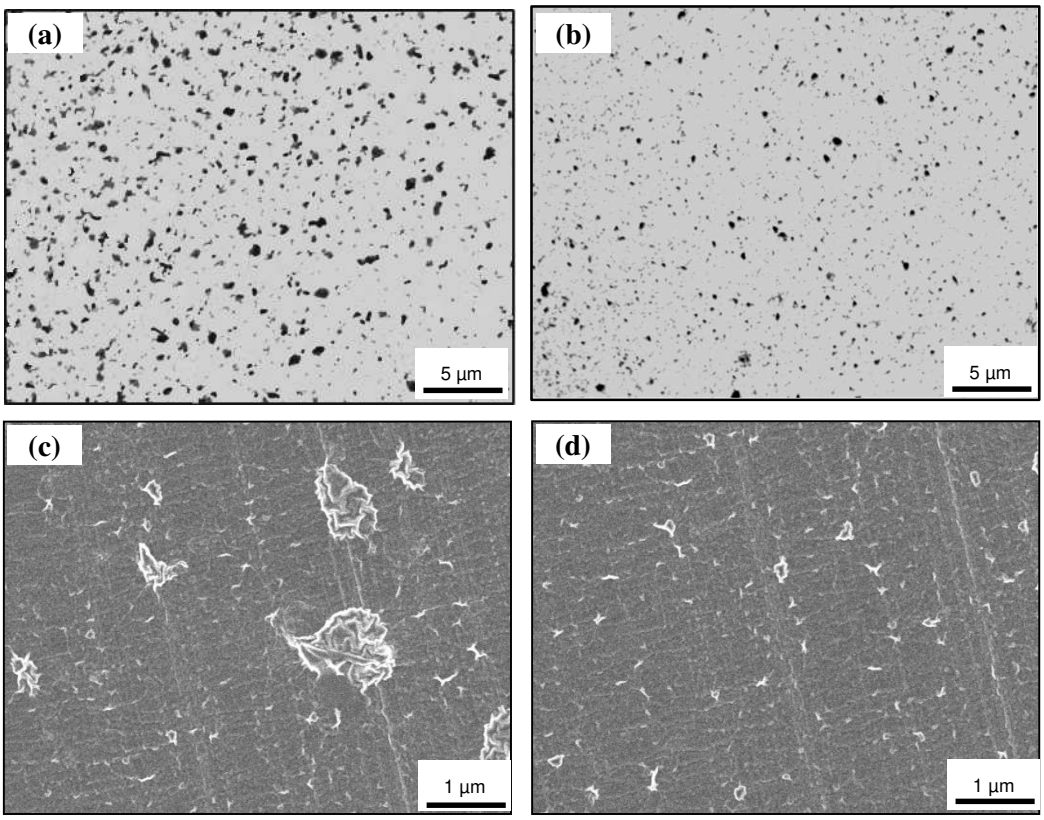

Figure 5

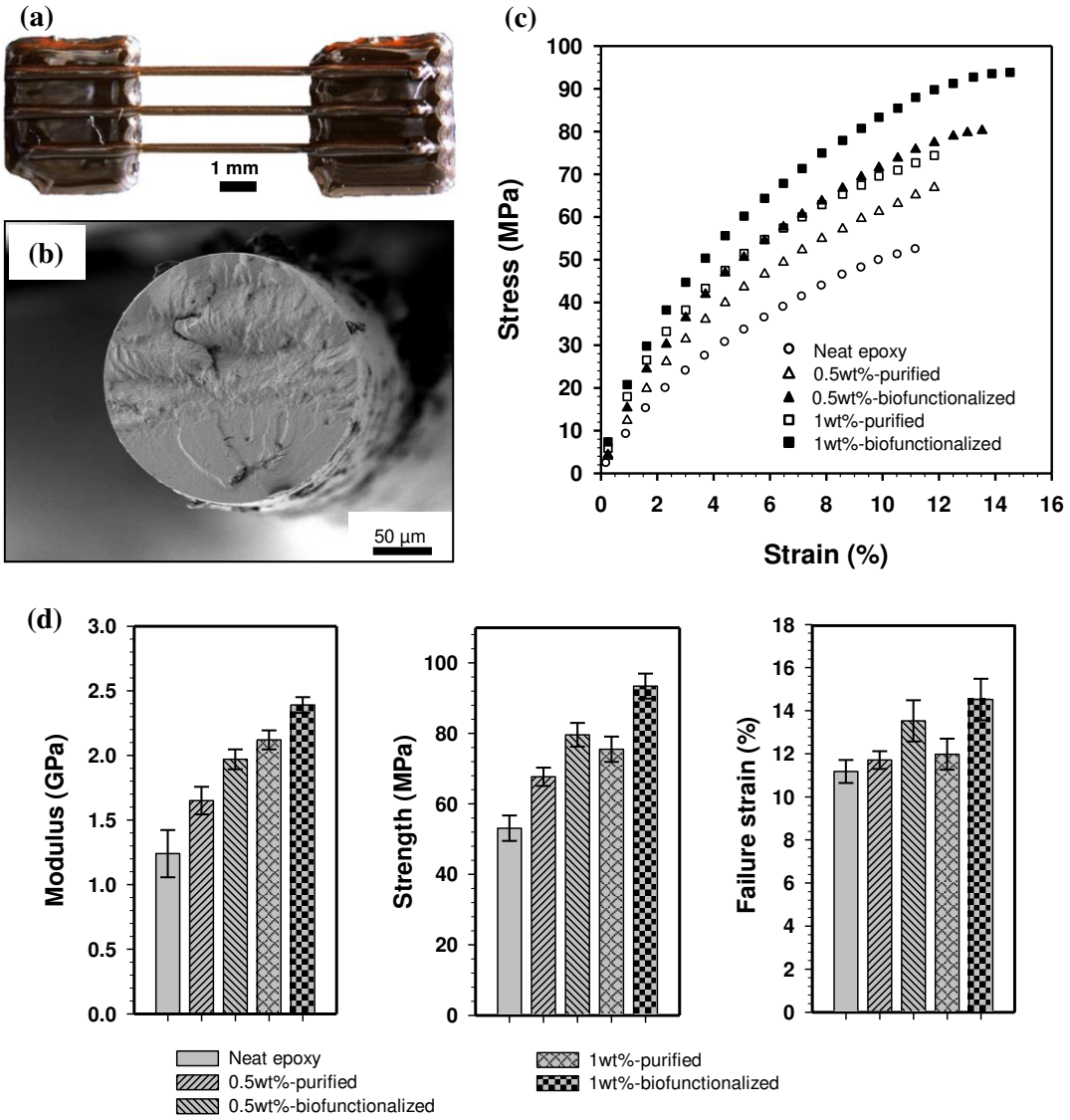
(a)
1 mm
(b)
50 µm
(c)
Stress (MPa)
Strain (%)
Neat epoxy
0.5wt%-purified
0.5wt%-biofunctionalized
1wt%-purified
1wt%-biofunctionalized
(d)
Modulus (GPa)
Strength (MPa)
Failure strain (%)
Neat epoxy
0.5wt%-purified
0.5wt%-biofunctionalized
1wt%-purified
1wt%-biofunctionalized

Figure 6

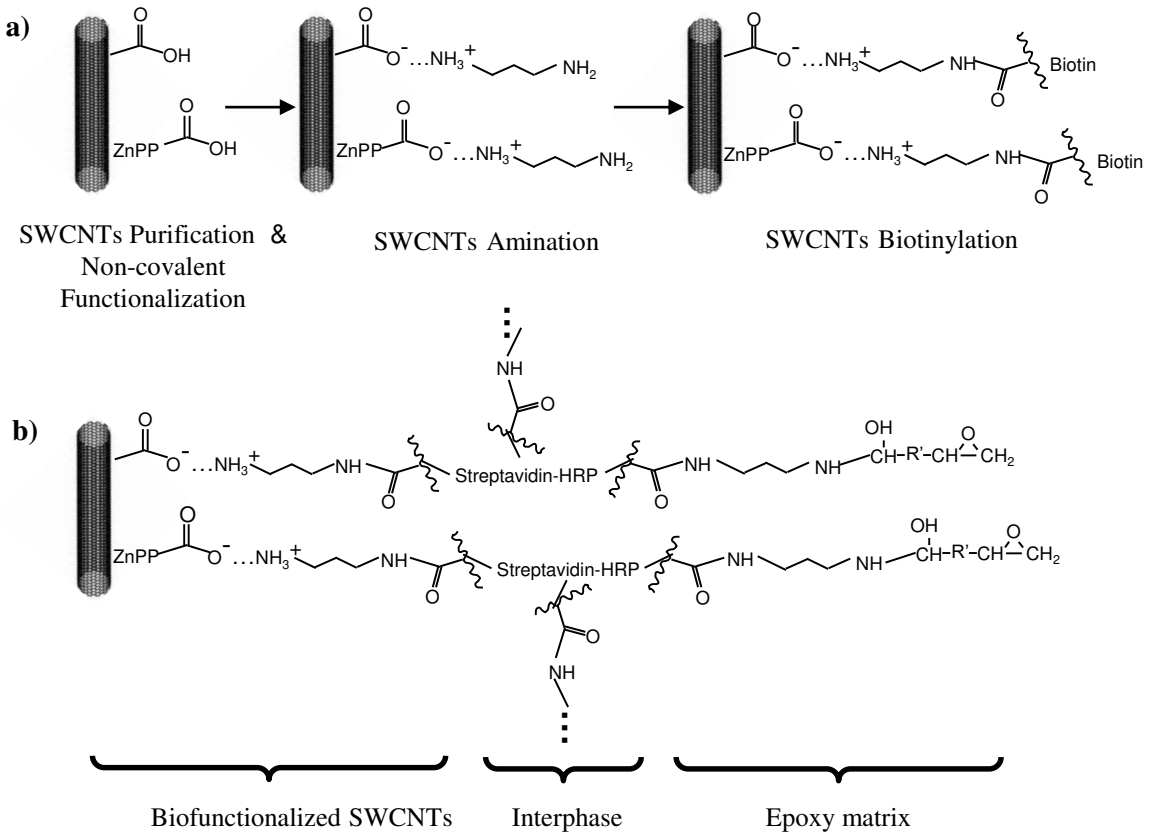

Figure 7